Ionizáló sugárzás hatására bekövetkező sejthalál, túlélési görbék

Mi a sejthalál?????

- Differenciált sejtek: a specifikus funkció elvesztése, destrukció
  - 100 Gy
- Proliferálódó sejtek: a reproduktív kapacitás elvesztése
  - 2 Gy

Sejthalál típusai

- Apoptózis
  - Belső, külső szignálok ndukálják
  - Szenzors (citokróm c, caspase 8, 9), effektors (caspase 3)
  - Pro-(p53, BAX, PUMA) és anti-apoptotikus (Bcl2, IAP)faktors
- Autofágia
  - Energia nyerés, sejthalál (Beclin1, p53, PTEN)
- Nekrózis
  - Szervezett folyamat???
- Senescence
  - Hayflick hatás
  - Telomér rövidülés
  - G1 ellenőrzési pont
- Mitotikus katasztrófa
  - Kromszóma aberrációk, G2 ellenőrzési pont

Hogyan halnak meg a sejtek???

Table 3.1 The characteristics of different types of cell death*

Type of cell death	Morphological changes			Biochemical features	Common detection methods
	Nucleus	Cell membrane	Cytoplasm		
Apoptosis	Chromatin condensation; nuclear fragmentation; DNA laddering	Blebbing	Fragmentation (formation of apoptotic bodies)	Caspase-dependent	Electron microscopy; TUNEL staining; annexin staining; caspase-activity assays; DNA-fragmentation assays; detection of increased number of cells in sub-G1/G0; detection of changes in mitochondrial membrane potential
Autophagy	Partial chromatin condensation; no DNA laddering	Blebbing	Increased number of autophagic vesicles	Caspase-independent; increased lysosomal activity	Electron microscopy; protein-degradation assays; assays for marker–protein translocation to autophagic membranes
Necrosis	Clumping and random degradation of nuclear DNA	Swelling; rupture	Increased vacuolation; organelle degeneration; mitochondrial swelling	–	Electron microscopy; nuclear staining (usually negative); detection of inflammation and damage in surrounding tissues
Senescence	Distinct heterochromatic structure (senescence-associated heterochromatic foci)	–	Flattening and increased granularity	SA-β-gal activity	Electron microscopy; SA-β-gal staining; growth-arrest assays
Mitotic catastrophe	Multiple micronuclei; nuclear fragmentation; dicentric chromosomes	–	–	Caspase-independent (at early stage) abnormal CDK1/cyclin B activation	Electron microscopy; assays for mitotic markers (MPM2); TUNEL staining

CDK1, cyclin-dependent kinase 1; SA-β-gal, senescence-associated galactose; TUNEL, terminal deoxynucleotidyl transferase dUTP nick end labelling.

*Adapted from Okada and Mak (2004). Adapted by permission from Macmillan Publishers Ltd.

Mikor halnak meg a sejtek???

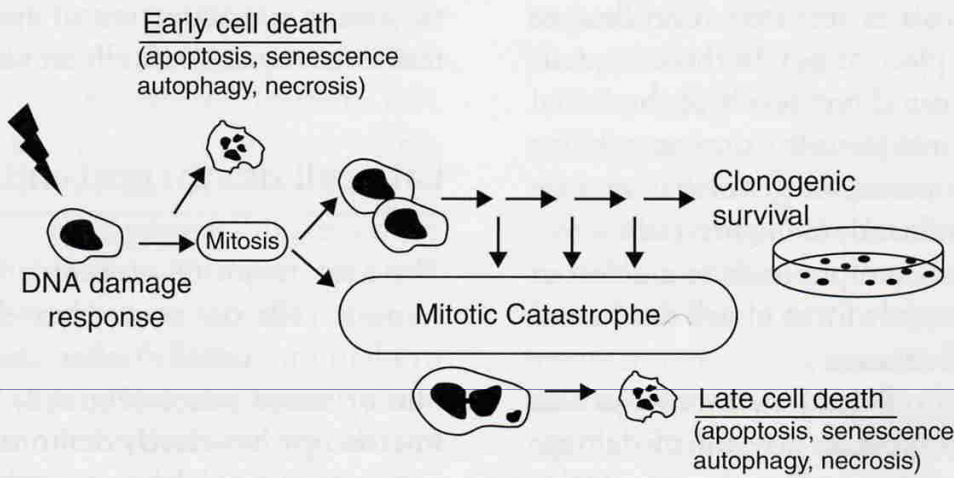

Figure 3.1 Schematic of cell death following irradiation. DNA damage induced by irradiation elicits activation of the DNA damage response (DDR – see Chapter 2), which leads to induction of cell-cycle checkpoints and DNA repair. In certain rare cells this response also induces apoptosis or other forms of cell death. However, in most cases cells die only after attempting mitosis. Remaining or improperly repaired DNA damage causes mitotic catastrophe, which subsequently leads to cell death. Mitotic catastrophe and cell death can take place after the first attempt at cell division, or after several rounds of proliferation. Consequently, this form of cell death is considered late cell death.

Pre- és poszt-mitotikus sejthalál

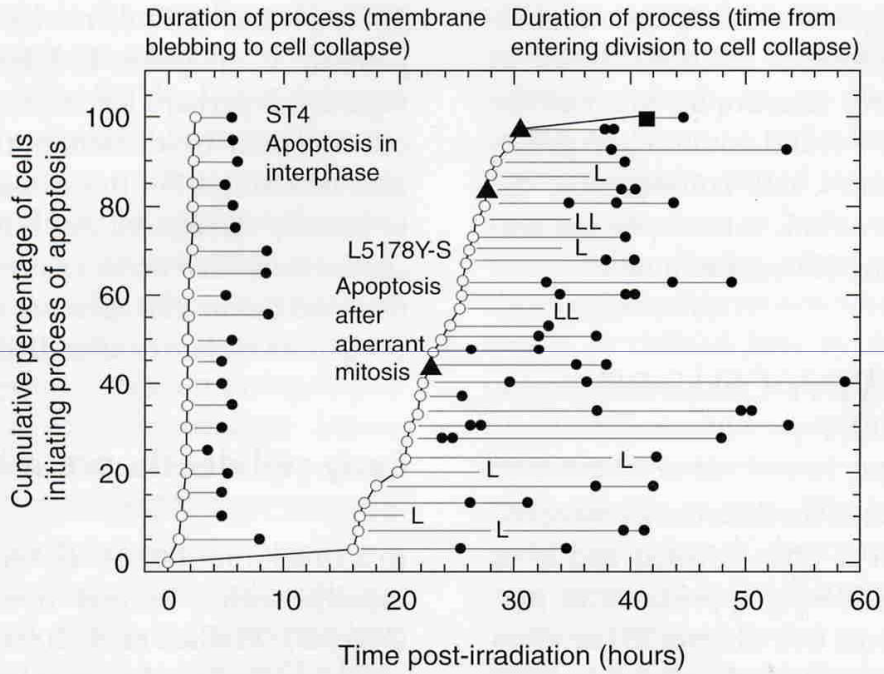

Figure 3.2 Data from Endlich *et al.* (2000) demonstrating early and late forms of cell death. The ST4 lymphoid cells die rapidly by apoptosis before mitosis. L5178Y-S cells also die by apoptosis following irradiation, but only after attempting to complete mitosis. In this case the initial DNA damage response is not sufficient to induce cell death and the cells die because of problems that occur during mitosis.

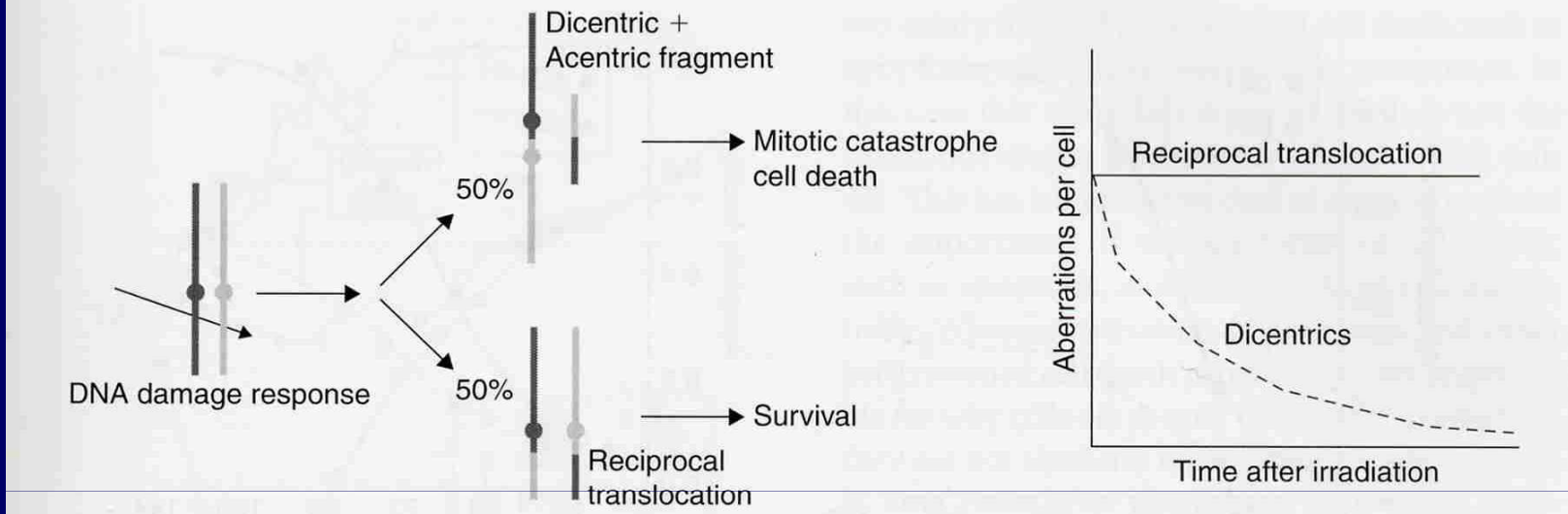

Figure 3.3 This figure, adapted from Brown and Attardi (2005), demonstrates the stochastic nature of cell death after irradiation. The DNA repair processes frequently lead to events in which chromosomes are not repaired correctly. It has been shown that irradiated cells produce approximately equal amounts of reciprocal translocations and dicentrics. The broken chromosomes in these cases are ligated to each other in a random or stochastic manner. Formation of a dicentric chromosome prevents proper mitosis and leads to cell death, whereas a reciprocal translocation that does not involve an important region of the genome is stable (sometimes for many decades). Thus, a population of irradiated cells will have approximately equal numbers of both types of aberrations and over time the cells with dicentrics will be lost owing to mitotic catastrophe-induced death. The initial amount of DNA damage and activation of the DNA damage response is the same in both types of cells but the outcome is very different. The outcome in this case is determined by the ability of the cells to avoid mitotic catastrophe. Adapted by permission from Macmillan Publishers Ltd.

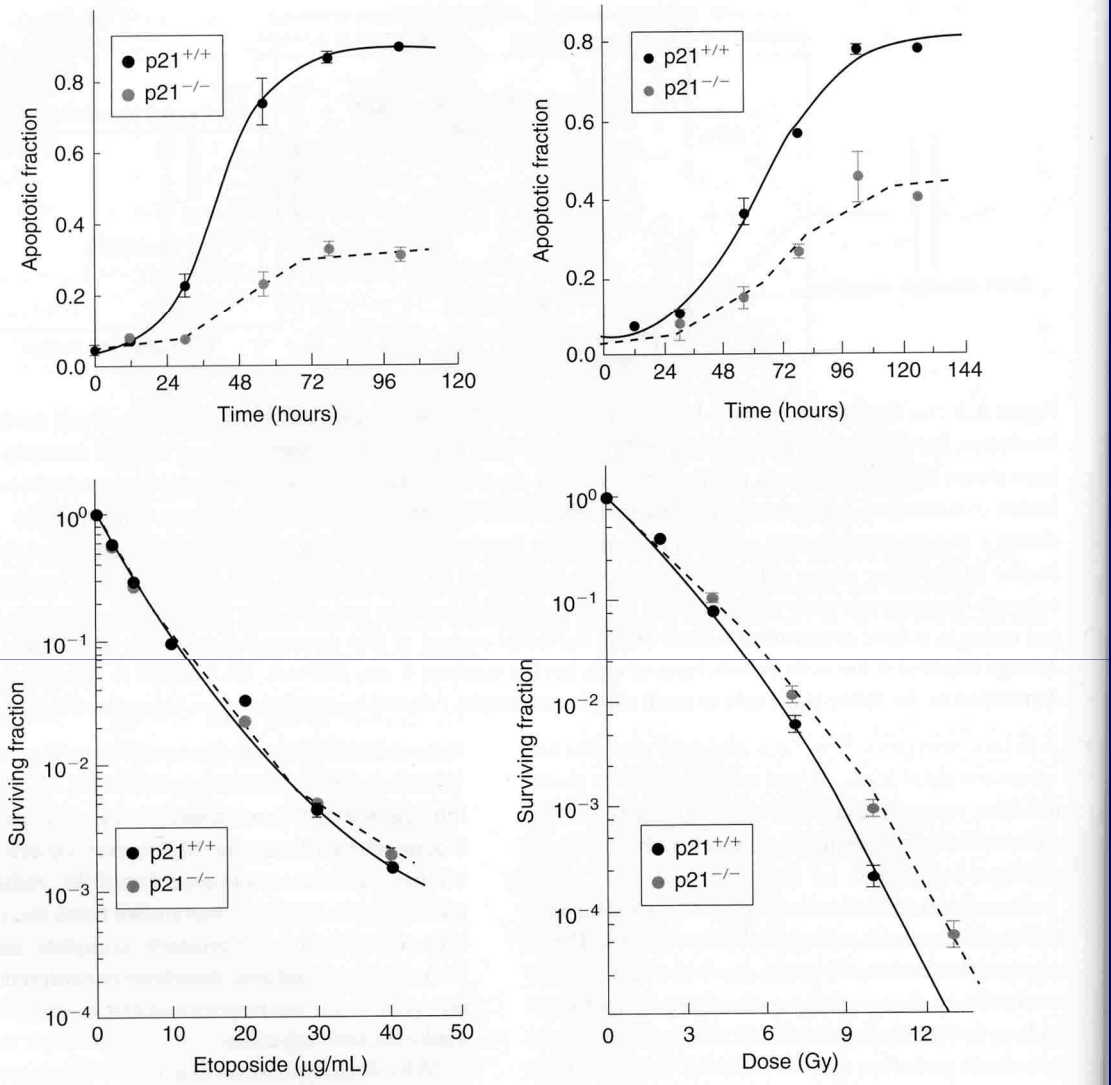

Figure 3.4 This figure, adapted from Wouters *et al.* (1997), demonstrates the discordance between assays of cell death and cell survival. The two cell lines differ only in the expression of the p21 cyclin-dependent kinase gene (*CDKN1A*). The p21 knockout cells show increased apoptosis after etoposide or irradiation (top panels) compared with the p21 wild-type cells. However, when assessed by clonogenic survival the p21 knockouts show a similar sensitivity to etoposide and a slight resistance to irradiation compared with the p21 wild-type cells. Here, apoptosis takes place after mitotic catastrophe and is just one mode of cell death that contributes to the loss of clonogenicity. Adapted with permission of American Association for Cancer Research.

A sejthalál típusa megszabja a sejthalál idejét

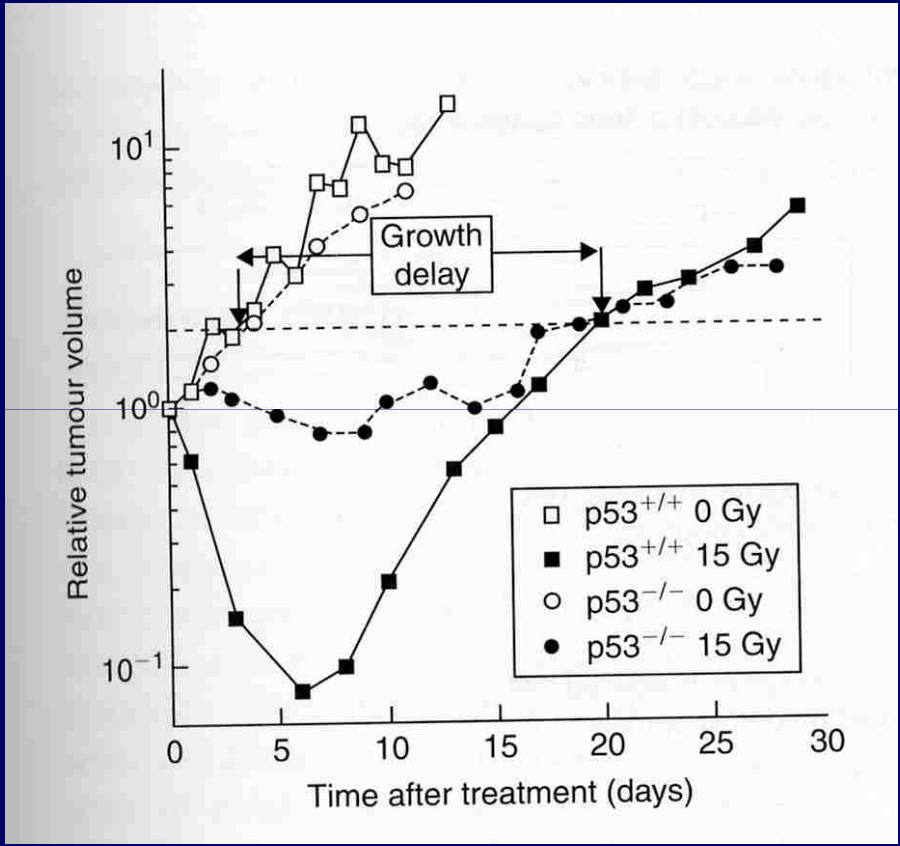

Figure 3.5 Although the mode of cell death may not affect the overall number of cells that die, it can dramatically affect the timing of their death. In this tumour regrowth experiment (from Brown and Wouters, 1999), tumours composed of p53 wild-type and knockout cells are irradiated and followed as a function of time. The unirradiated tumours grow at a similar rate. However, the p53 wild-type tumours undergo rapid apoptosis after irradiation and the tumours thus also shrink rapidly in size. The p53 knockout tumours do not undergo apoptosis and thus are considerably larger after irradiation during this first week. However, the total regrowth delay (measured when tumours reach twice their starting size) is identical for the two tumour types. This indicates that the total number of cells killed by irradiation is the same in both tumour types. In this case apoptosis alters the speed at which the cells die, but does not affect the total number of initially irradiated cells that will eventually die. Adapted with permission of American Association for Cancer Research.

Mitotikus katasztrófa során a sejthalál ideje és típusa változó

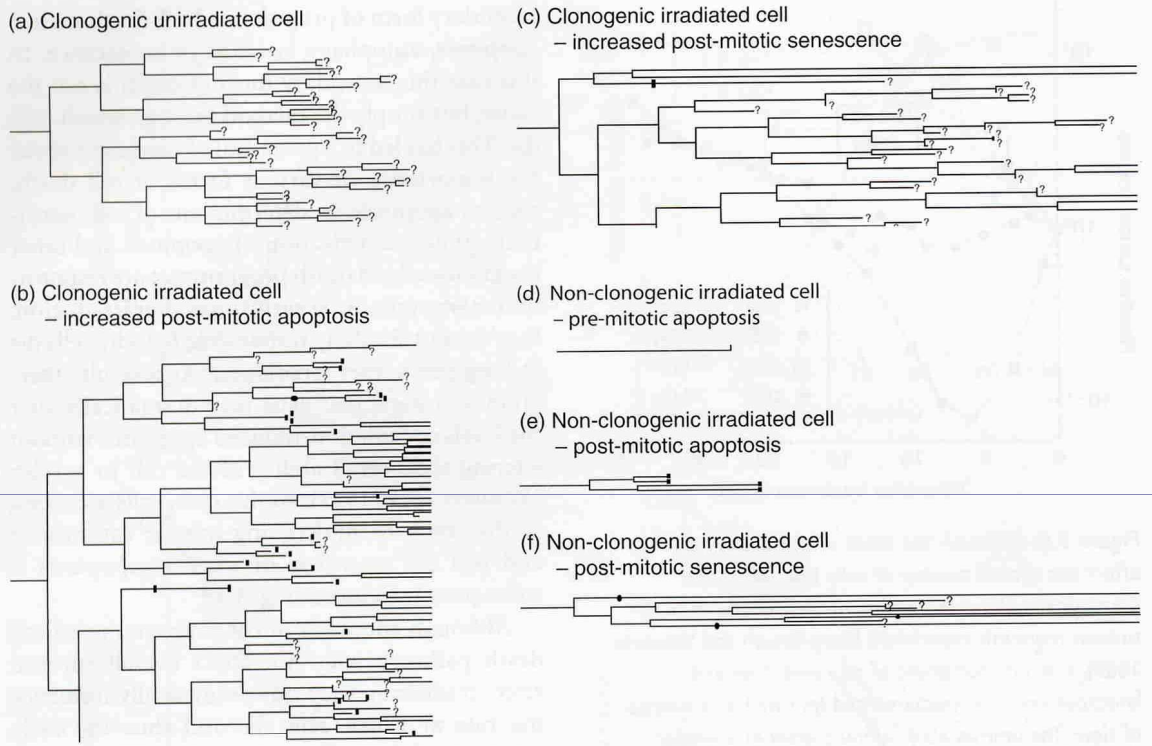

Figure 3.6 This figure, adapted from Forrester *et al.* (1999), tracks the fate of several irradiated cells as a function of time (left to right) following exposure to radiation. (a) An unirradiated cell is shown as an example. Each cell division is indicated by a split of one line into two. After six or seven divisions enough cell progeny have been created to produce a colony that can be scored as a survivor. The initial cell is thus said to be clonogenic. Two cells that survive irradiation and eventually form colonies are shown in (b) and (c). In (b), the first division produces two daughter cells that both progress to mitosis and divide producing four cells. One of these four cells dies by apoptosis. Another one undergoes several more divisions but produces progeny that all eventually die. The other two cells both produce many surviving progeny that contribute to the long-term clonogenic potential of the initially irradiated cell. Note, that many of the progeny die in this case even though the initial cell has 'survived'. In (c) the irradiated cell is also clonogenic. In this case, one of the first two daughter cells produces cells which all eventually undergo senescence. Irradiated cells that are non-clonogenic are shown in (d), (e) and (f). In (d), a cell dies by apoptosis before mitosis. In (e) cells die by apoptosis after completing two divisions and in (e) cells undergo senescence after undergoing one or more mitoses. Adapted with permission of American Association for Cancer Research.

Nem DNS célpontú hatások

Bystander sejthalál

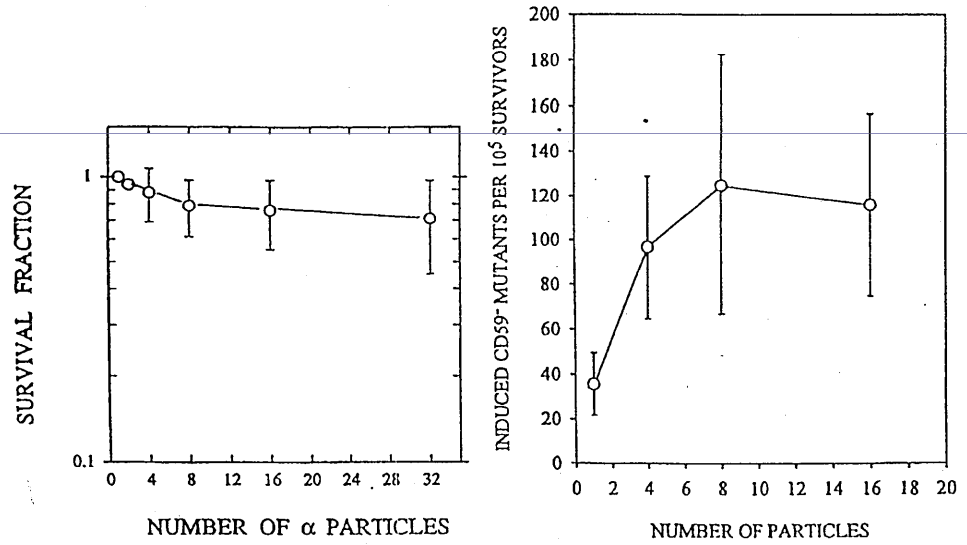

Fig. 4. Cell survival and induced frequency of mutations in A_L cells in which the cytoplasm was irradiated with an exact number of α-particles from a precision microbeam irradiator. The background mutation frequency was 43 ± 15 mutants per 10^5 survivors. Data from Wu *et al.* (57).

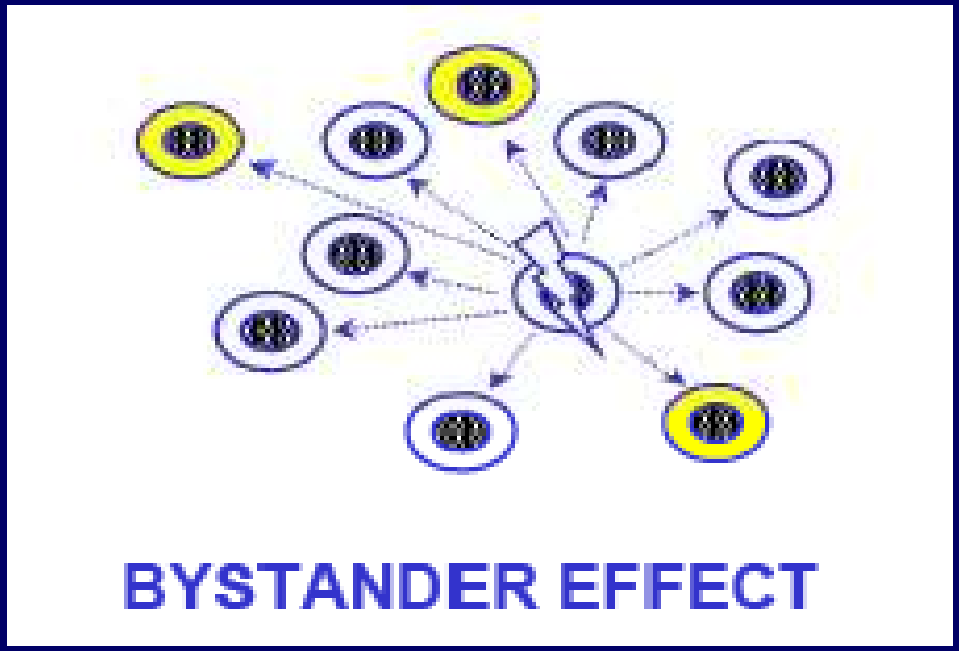

- Sejthalál
- Mutációk

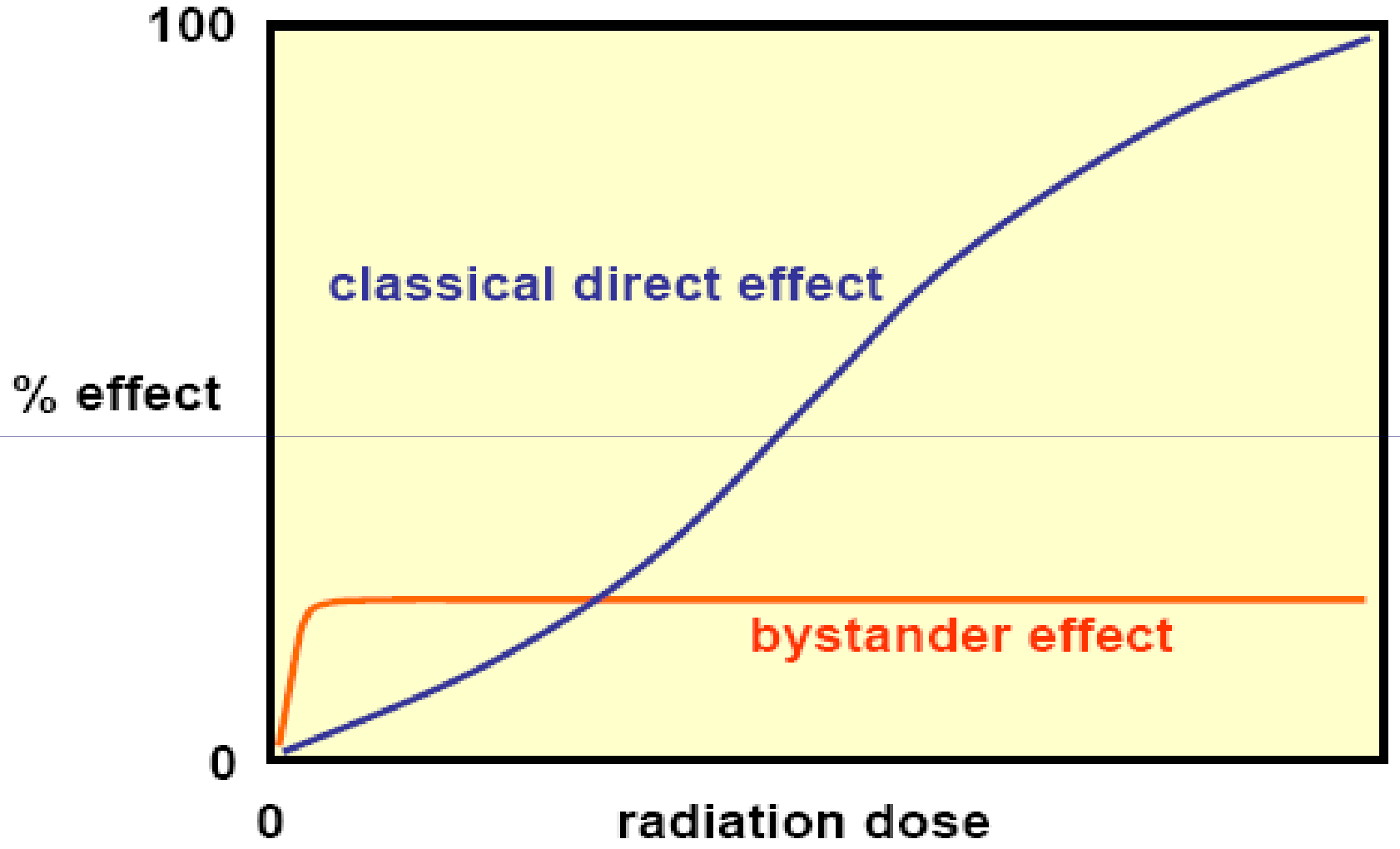
100
% effect
0
0
radiation dose
classical direct effect
bystander effect

A sejthalál követése

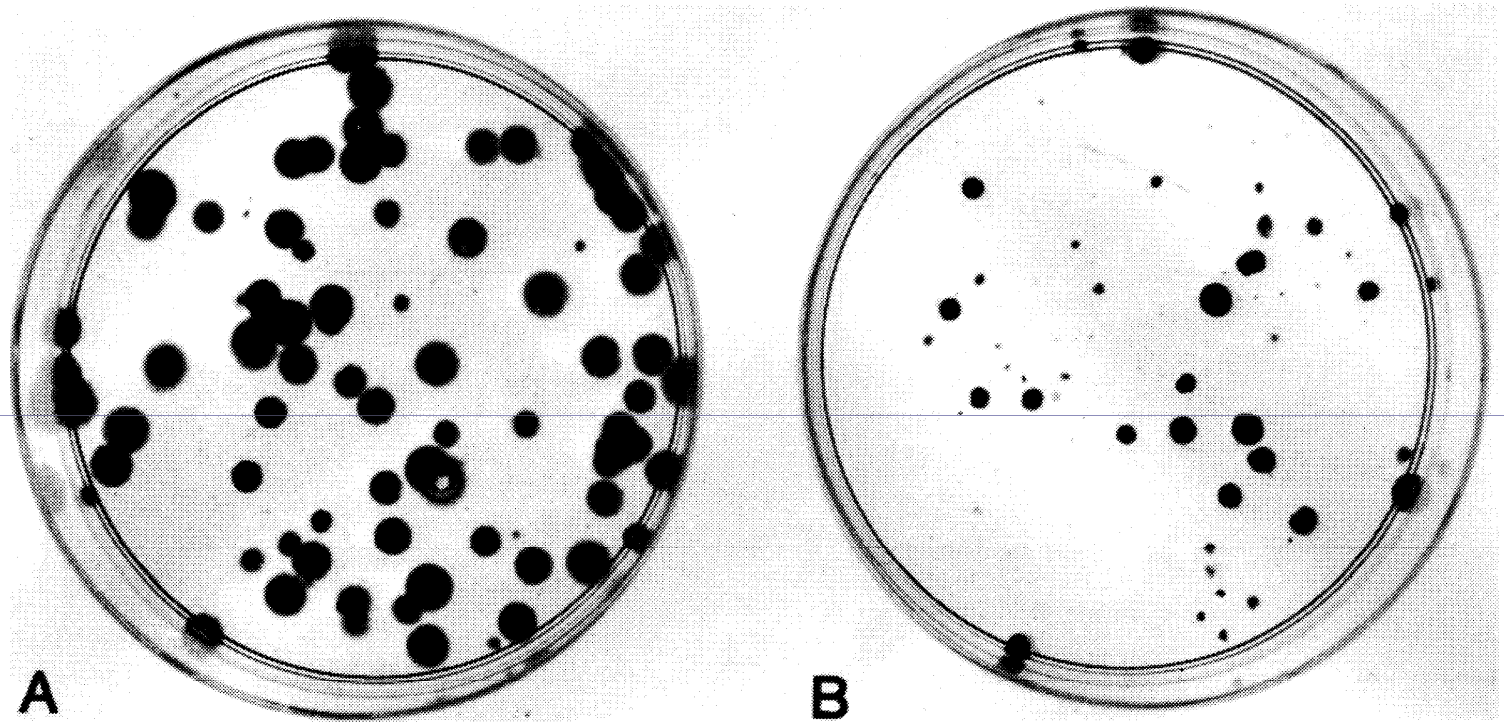

Figure 3.1. Colonies obtained with Chinese hamster cells cultured in vitro. **A:** In this unirradiated control dish 100 cells were seeded and allowed to grow for 7 days before being stained. There are 70 colonies; therefore the plating efficiency is 70/100, or 70%. **B:** Two thousand cells were seeded and then exposed to 800 rad (8 Gy) of x-rays. There are 32 colonies on the dish. Thus:
Surviving fraction = Colonies counted [colonies seeded x (PE/100)]
= 32/2000x .7
= 0.023

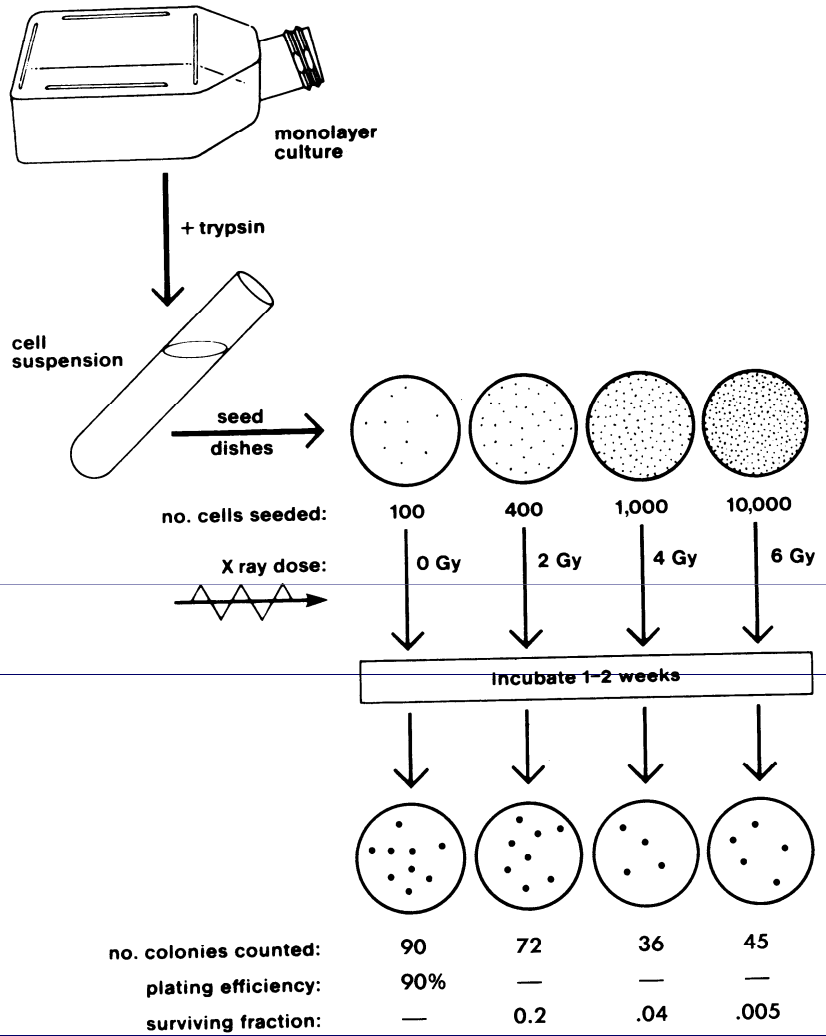

Figure 3.2. The cell culture technique used to generate a cell-survival curve. Cells from a stock culture are prepared into a single-cell suspension by trypsinization, and the cell concentration is counted. Known numbers of cells are inoculated into petri dishes and irradiated. They then are allowed to grow until the surviving cells produce macroscopic colonies that can be counted readily. The number of cells per dish initially inoculated varies with the dose, so that the number of colonies surviving is in the range that can be counted conveniently. Surviving fraction is the ratio of colonies produced to cells plated, with a correction necessary for plating efficiency (*i.e.*, for the fact that not all cells plated grow into colonies, even in the absence of radiation).

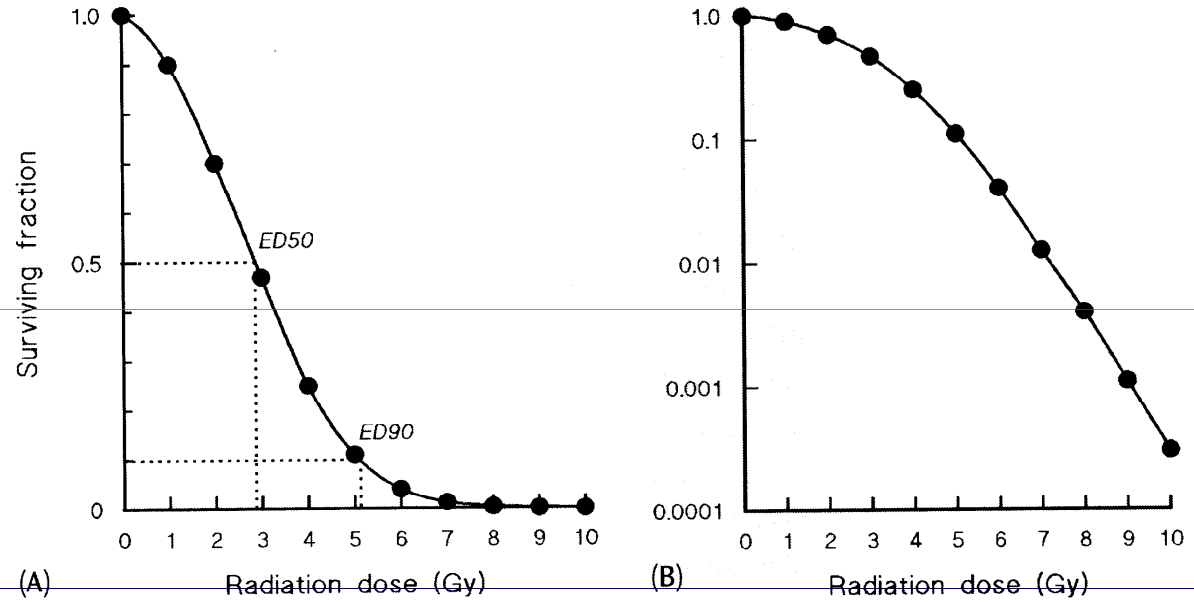

Figure 6.3 *A typical cell survival curve for cells irradiated in tissue culture, plotted (A) on a linear survival scale. (B) Shows the same data plotted on a logarithmic scale.*

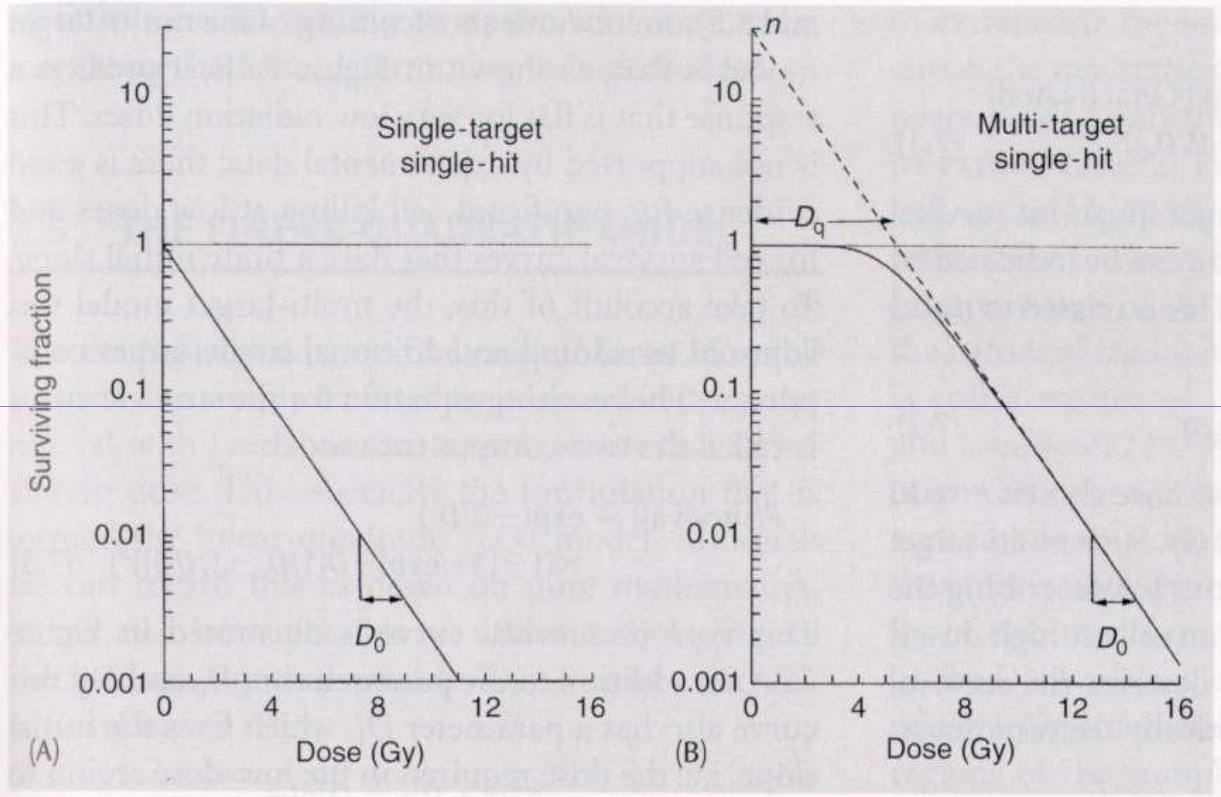

Figure 7.1 *The two most common types of target theory. (A) Single-target inactivation; (B) multi-target inactivation.*

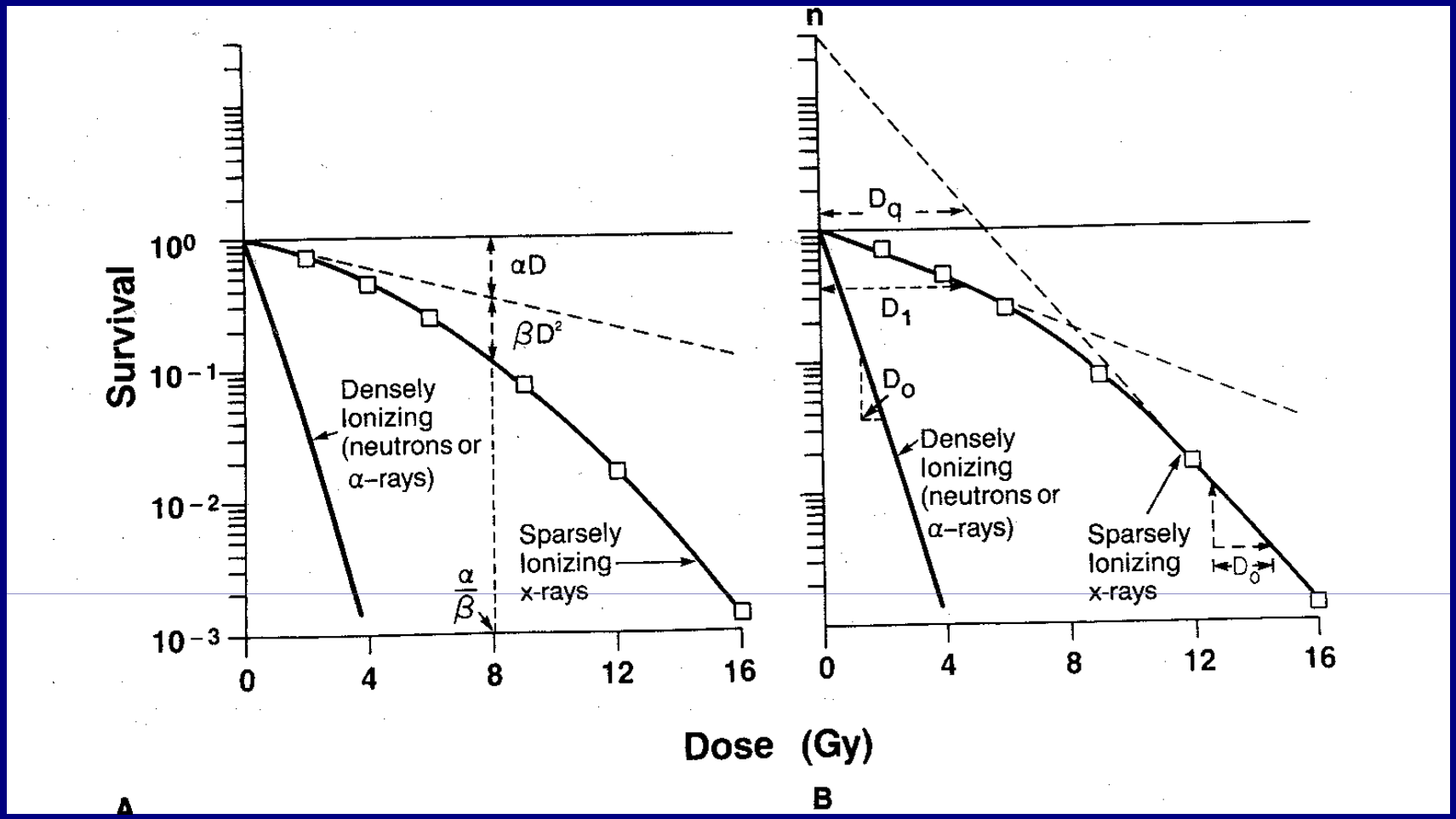

n – extrapolációs szám; D_q – kvázi küszöbdózis; D_0 – 0,37-re csökkenti a túlélést. $Log_e n = D_q/D_0$

$E=\alpha D+\beta D^2$; Ha az α és β egyenlő arányban járul hozzá a hatáshoz

$\alpha D=\beta D^2$, $D=\alpha/\beta$; BED=nd[1+d/α/β]

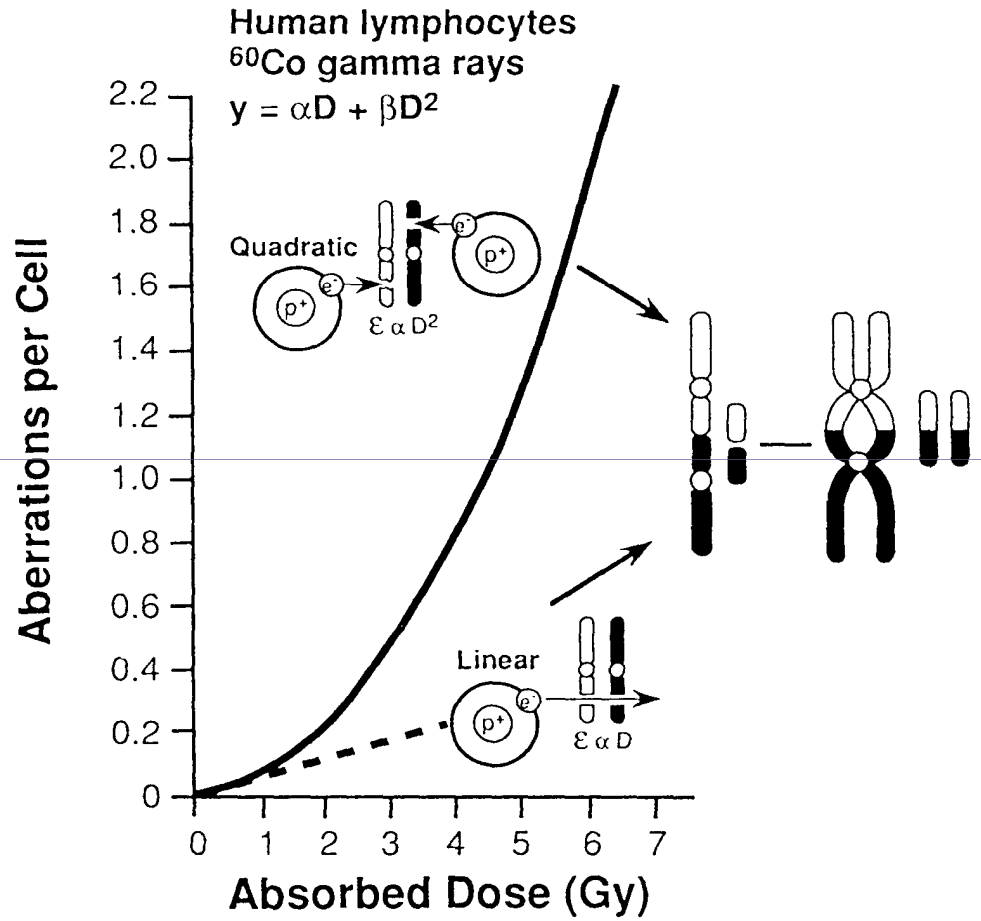

Figure 2.11. The frequency of chromosomal aberrations (dicentrics and rings) is a linear-quadratic function of dose because the aberrations are the consequence of the interaction of two separate breaks. At low doses, both breaks may be caused by the same electron; the probability of an exchange aberration is proportional to dose (D). At higher doses, the two breaks are more likely to be caused by separate electrons. The probability of an exchange aberration is proportional to the square of the dose (D^2).

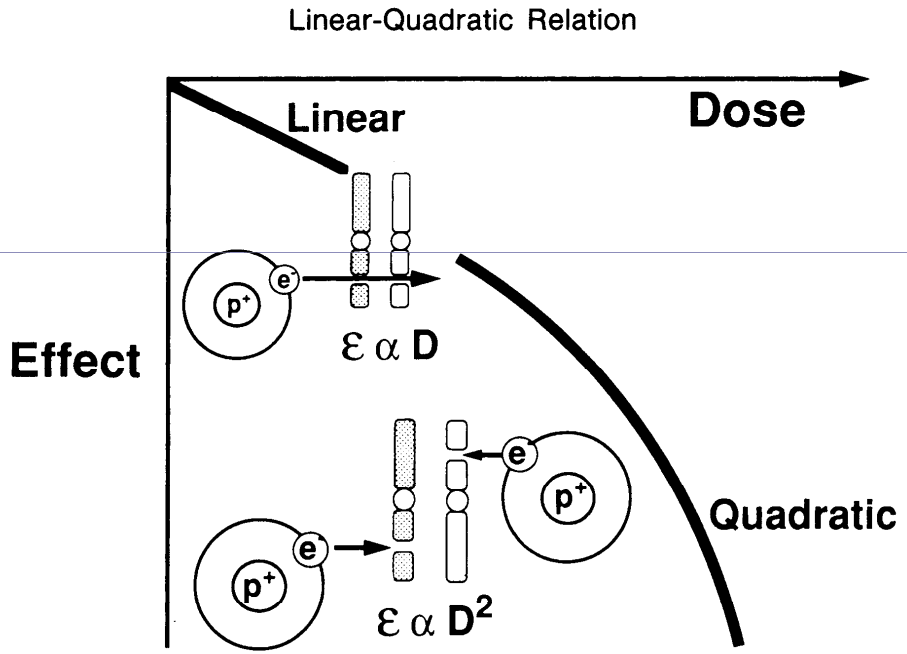

Figure 3.6. Relationship between chromosome aberrations and cell survival. Cells that suffer exchange-type chromosome aberrations (such as dicentric) are unable to survive and continue to divide indefinitely. At low doses, the two chromosome breaks are the consequence of a single electron set in motion by the absorption of x- or γ-rays. The probability of an interaction between the breaks is proportional to dose; this is the linear portion of the survival curve. At higher doses, the two chromosome breaks may result also from two separate electrons. The probability of an interaction is then proportional to the square of the dose. The survival curve bends if the quadratic component dominates.

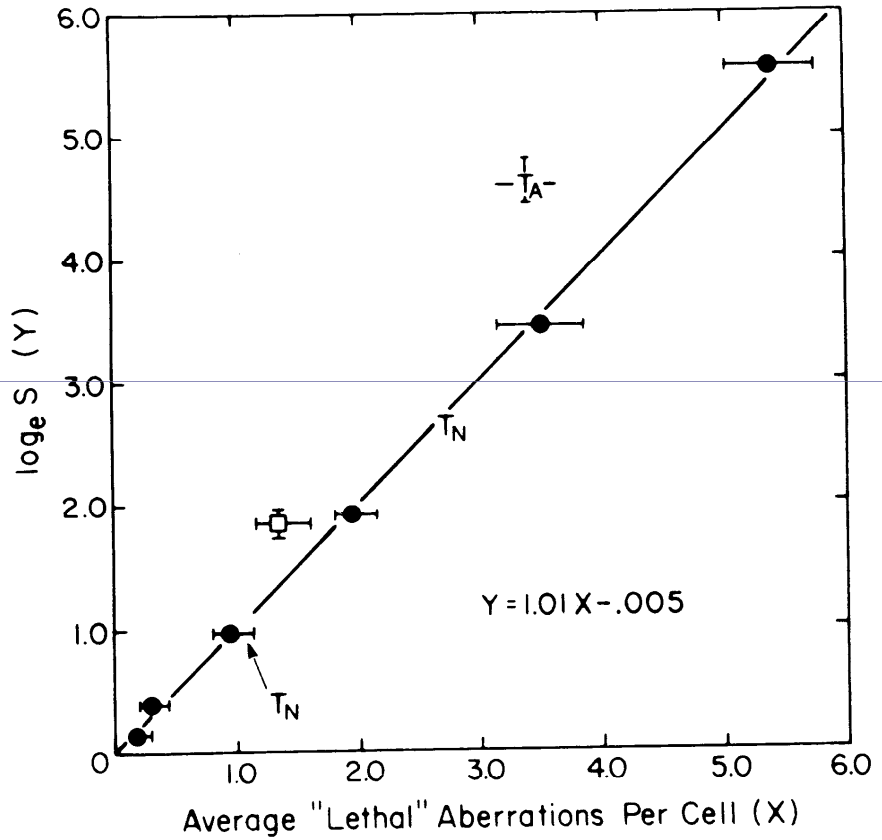

Figure 3.5. Relationship between the average number of "lethal" aberrations per cell (*i.e.*, asymmetric exchange-type aberrations such as dicentrics and rings) and the log of the surviving fraction in AC 1522 normal human fibroblasts exposed to x-rays. There is virtually a one-to-one correlation. (From Cornforth MN, Bedford JS: A quantitative comparison of potentially lethal damage repair and the rejoining of interphase chromosome breaks in low passage normal human fibroblasts. Radiat Res 111:385–405, 1987, with permission.)

Letális potenciálisan letális károsodás modell

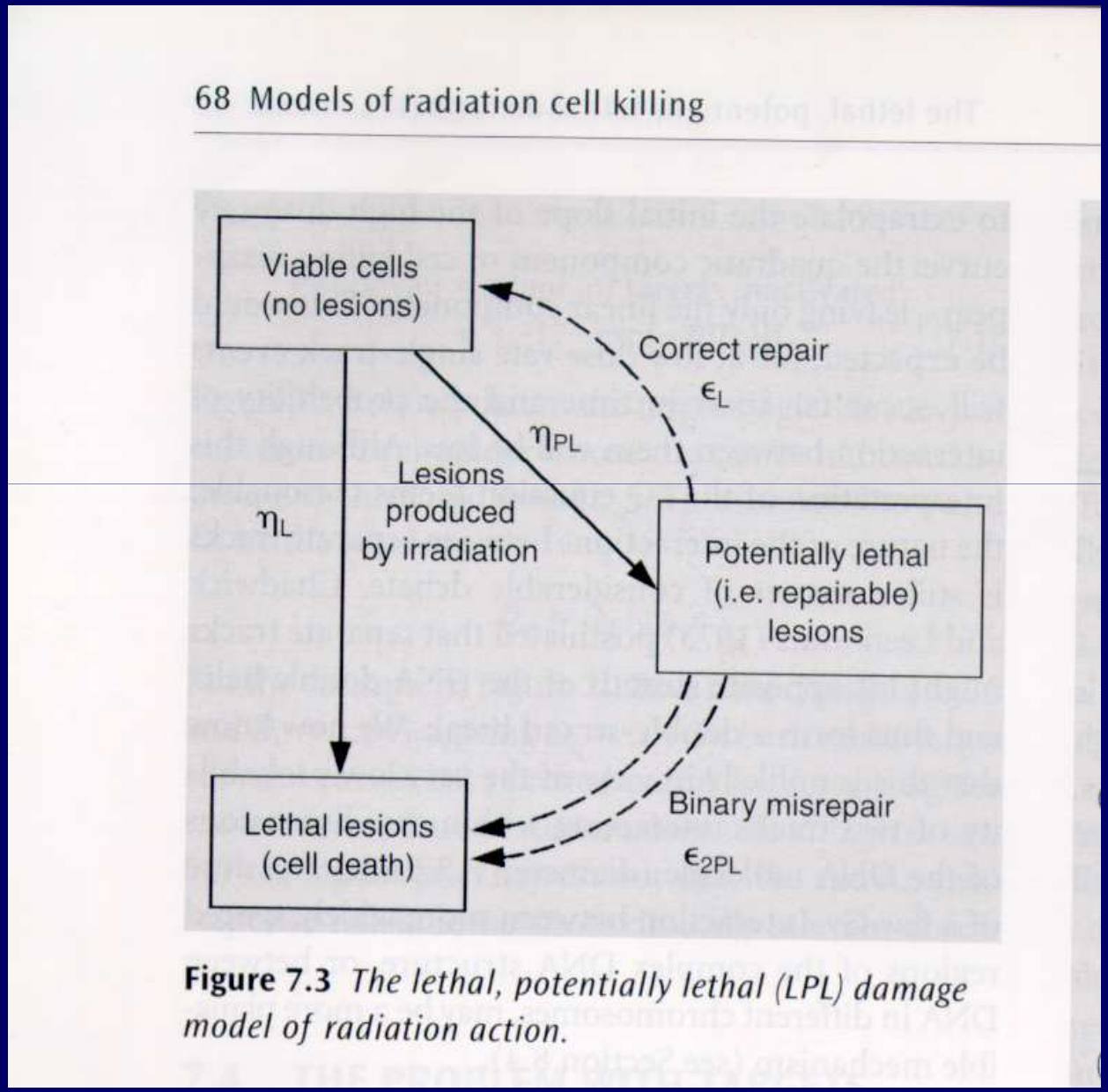

Figure 7.3 *The lethal, potentially lethal (LPL) damage model of radiation action.*

Letális potenciálisan letális károsodás modell

Repair telítési modell

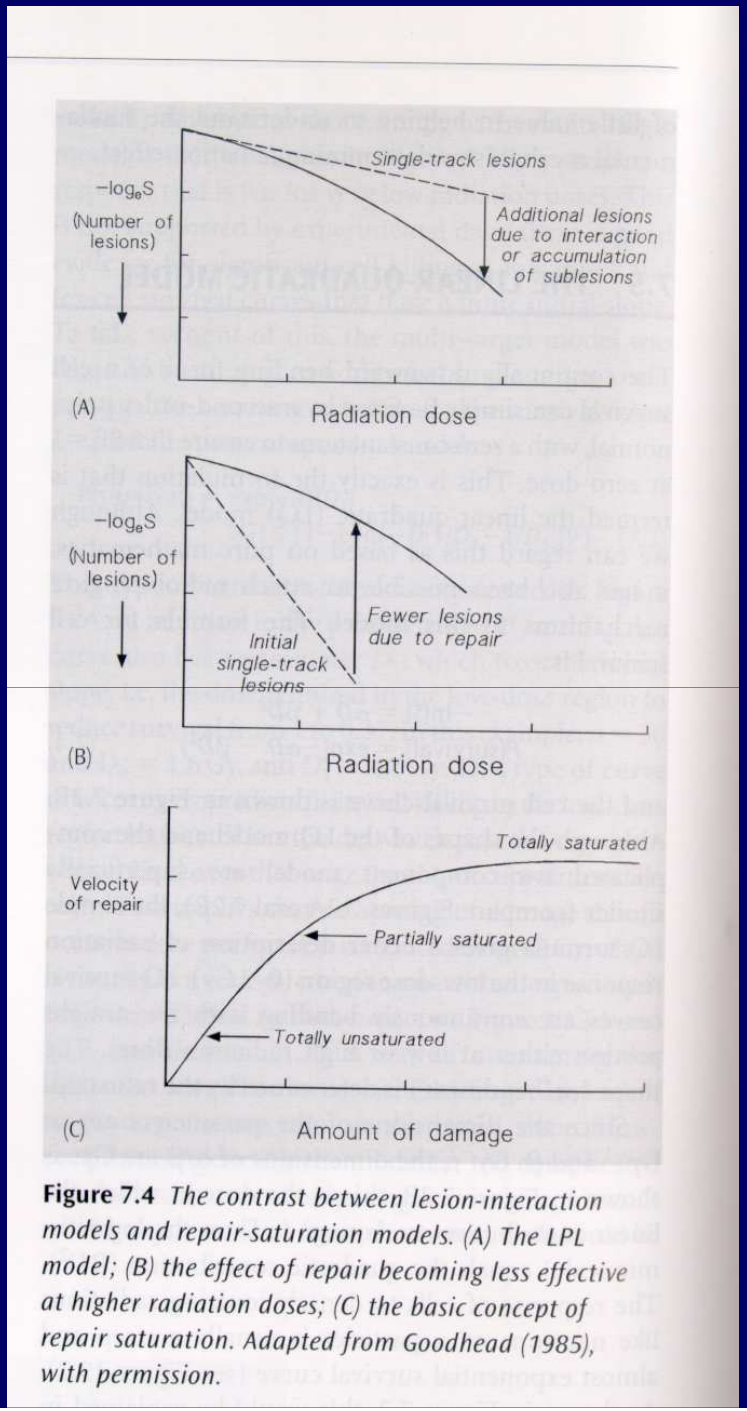

Figure 7.4 *The contrast between lesion-interaction models and repair-saturation models. (A) The LPL model; (B) the effect of repair becoming less effective at higher radiation doses; (C) the basic concept of repair saturation. Adapted from Goodhead (1985), with permission.*

Table 7.1 *Different interpretations of radiobiological phenomena by lesion-interaction and saturable-repair models*

Observation	Explanation	
	Lesion interaction	**Repair saturation**
Curved dose–effect relationship	Interaction of sublesions	Saturation of capacity to repair sublesions
Split-dose recovery	Repair of sublesions (sublethal damage repair)	Recovery of capacity to repair sublesions
RBE increase with LET	More non-repairable lesions at high LET	High-LET lesions are less repairable
Low dose rate is less effective	Repair of sublesions during irradiation	Repair system not saturating

Adapted from Goodhead (1985).

Lineáris-kvadratikus-köb modell

$S = \alpha D + \beta D^2 - \gamma D^3$

Emlős sejtek túlélési görbéje

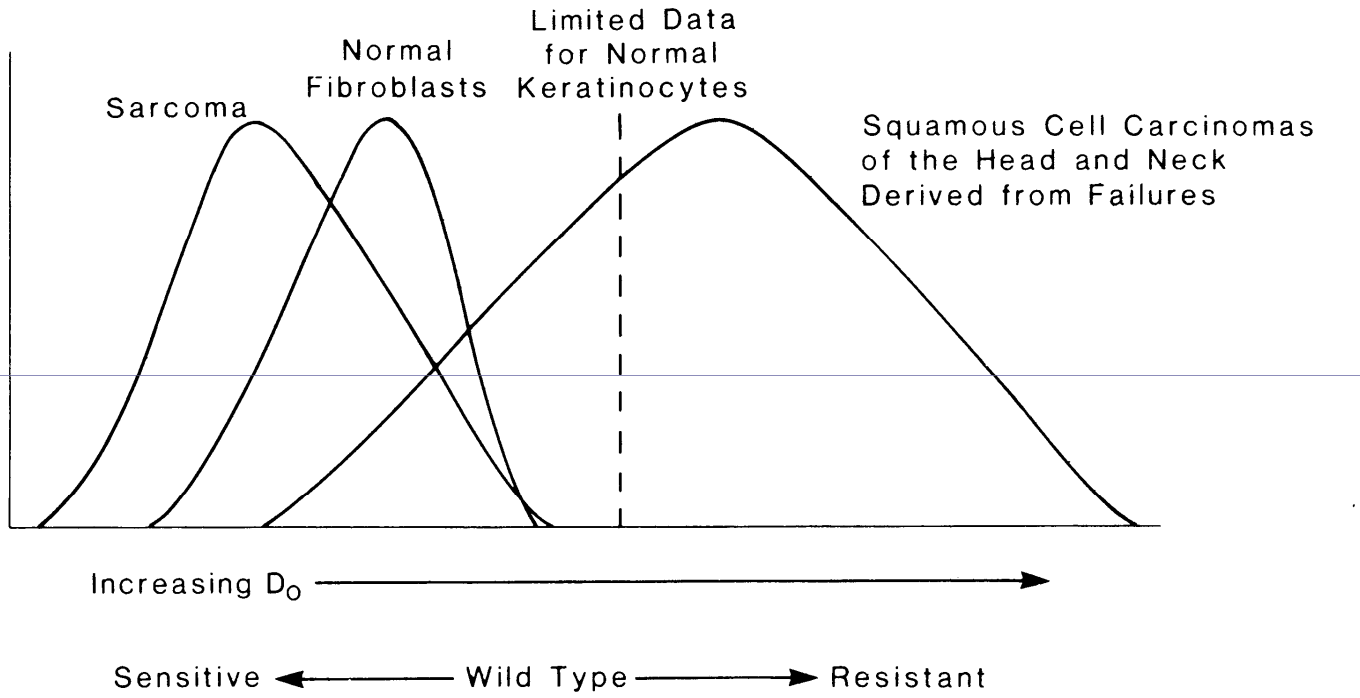

Figure 3.8. Summary of D_0 values for cells of human origin grown and irradiated *in vitro*. Cells from human tumors tend to have a wide range of radiosensitivities, which brackets the radiosensitivity of normal human fibroblasts. In general, squamous-cell carcinoma cells are more resistant than sarcoma cells, but the spectra of radiosensitivities are broad and overlap. (Courtesy of Dr. Ralph Wechselbaum.)

A túlélési görbe alakja és a sejtpusztulás mechanizmusa

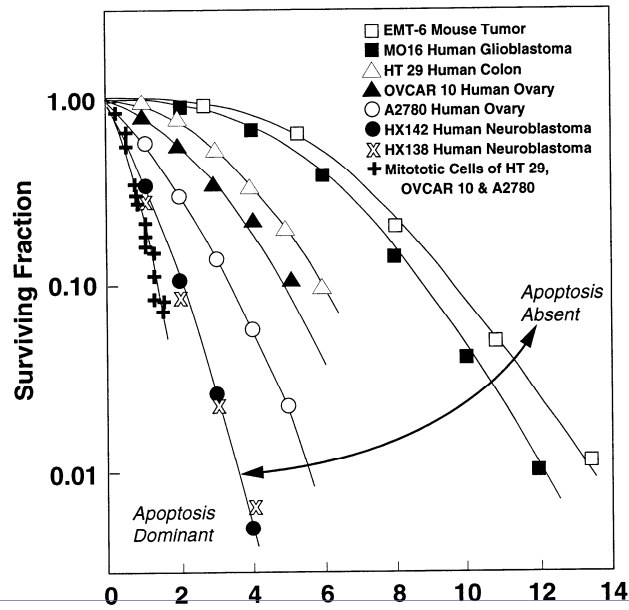

A

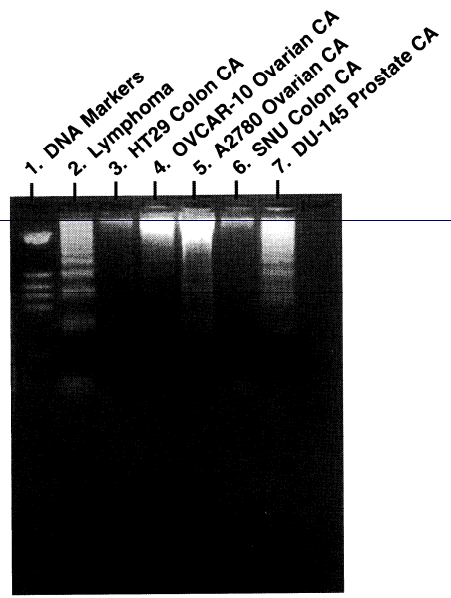

B

Figure 3.9. A: Compilation of survival curves for asynchronous cultures of a number of cell lines of human and rodent origin. Note the wide range of radiosensitivity (most notably the size of the shoulder) between mouse EMT6 cells, the most resistant, and two neuroblastoma cell lines of human origin (the most sensitive). The cell-survival curve for mitotic cells is very steep, and there is little difference in radiosensitivity for cell lines that are very different in asynchronous culture. (Data compiled by Dr. J. D. Chapman, Fox Chase Cancer Center, Philadelphia.) **B:** DNA purified from various cell lines (survival curves shown in Fig. 3.9A) 18 hours after irradiation with 10 Gy and electrophoresed for 90 minutes at 6 V/cm. Note the broad variation in the amount of "laddering"—which is characteristic of an apoptotic death. In this form of death, double-strand breaks occur in the liner regions between nucleosomes, to produce DNA fragments that are multiples of about 185 base pairs. Note that cell lines that show prominent laddering are radiosensitive. (Gel prepared by Drs. S. Biade and J.D. Chapman, Fox Chase Cancer Center, Philadelphia.)

A sugárérzékenység genetikai háttere

Ataxia telangiectasia	ATM
Basal cell nevoid syndrome	*PTCH* (Patched) gén
Cockayne's syndrome	DNS repair
Down syndrome	21 triszomia
Fanconi's anemia	13 gén, repair
Gardner's syndrome	APC gén
Nijmegan breakage syndrome	NBS
Usher's syndrome	10 gén

TABLE 3.1. *Inherited Human Syndromes Associated with Sensitivity to X-Rays*

Frakcionált besugárzás

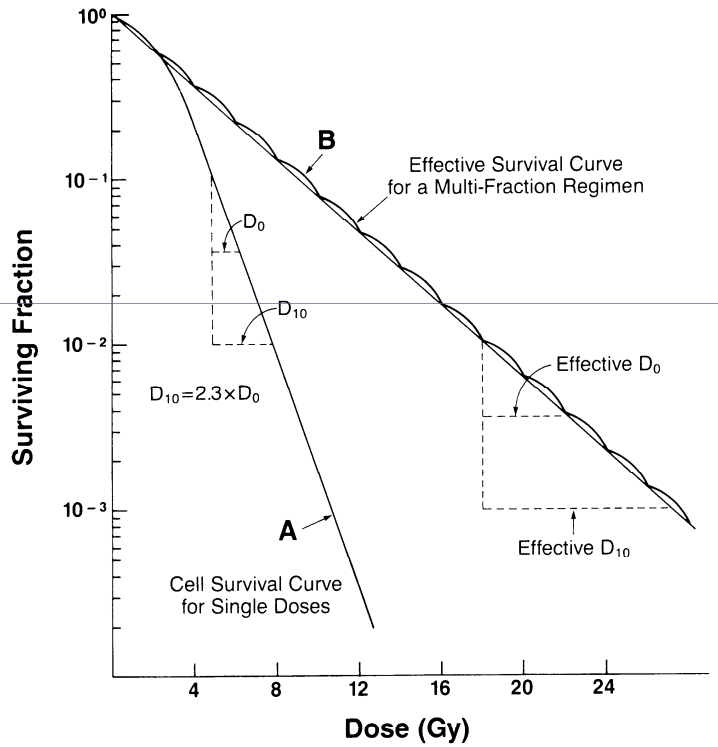

Figure 3.10. The concept of an "effective" survival curve for a multifraction regimen is illustrated. If the radiation dose is delivered in a series of equal fractions separated by time intervals sufficiently long for the repair of sublethal damage to be complete between fractions, the shoulder of the survival curve is repeated many times. The effective dose–survival curve is an exponential function of dose, that is, a straight line from the origin through a point on the single-dose survival curve corresponding to the daily dose fraction (*e.g.*, 2 Gy). The dose resulting in one decade of cell killing (D_{10}) is related to the D_0 by the expression $D_{10} = 2.3\ D_0$.

Mikroorganizmusok sugárérzékenysége

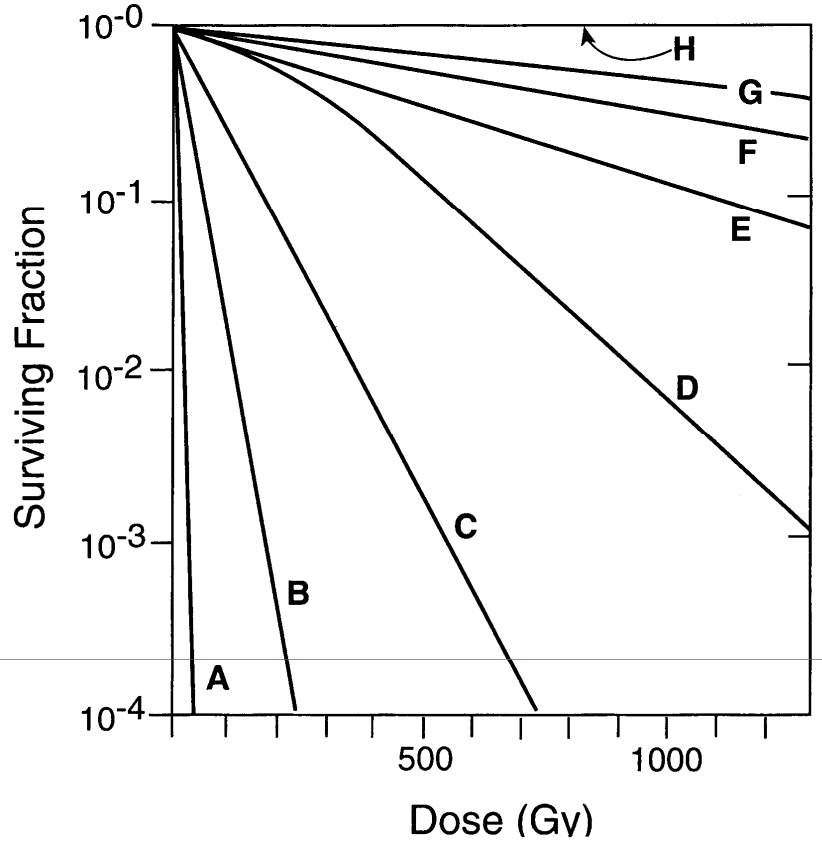

Figure 3.11. Survival curves for mammalian cells and for a variety of microorganisms, including *Escherichia coli*, yeast, and *Micrococcus radiodurans*. It is evident that mammalian cells are exquisitely radiosensitive compared with microorganisms, principally because they have a much larger DNA content, which represents a bigger "target" for radiation damage. **A**, mammalian cells; **B**, *E. coli*; **C**, *E. coli* B/r; **D**, yeast; **E**, phage staph E; **F**, *B. megatherium*; **G**, potato virus; **H**, *Micrococcus radiodurans*.

- A lineáris-kvadratikus modell a legelfogadottabb a dózis-hatás görbe modellezésére.
- Az α/β érték egyenlő azzal a dózissal, amikor az α és a β tényező egyenlőmértékben járul hozzá a hatáshoz
- A sejthalál szempontjából a DNS a fő célpont
- A sejtek leggyakrabban mitotikus katasztrófa következtében hallnak meg, az apoptózis viszonylag ritka
- Limfociták, timociták, oocyták, spermatogoniumok kizárólag apoptózissal pusztulnak el
- Az sugárzás-indukálta apoptózisra érzékeny sejtek sugárérzékenyek
- A kétláncú DNS repair hibái sugárérzékenységhez vezetnek
- Emlős (emberi) sejtek sugárérzékenyebbek, mint a mikroorganizmusok